

ELECTRONIC SUPPLEMENTARY INFORMATION (ESI) FOR:

Ln(III)-Containing Polyoxomolybdates based on β -{Mo₈O₂₈}: Microwave synthesis, Optical and Magnetic properties

Yanxin Zhao, Shumin Chen, Yanfang Ji, Vikram Singh, Pengtao Ma, Jingkun Lu, Jingyang Niu* and Jingping Wang*

*Key Laboratory of Polyoxometalate Chemistry of Henan Province Institute of Molecular and Crystal Engineering
College of Chemistry and Chemical Engineering Henan University, Kaifeng, Henan 475004 (P. R. China)*

Contents

- 1. Experiment instruments and reagents**
- 2. Synthesis of compounds**
- 3. Infrared spectroscopy analysis of compounds**
- 4. UV-Vis spectroscopy of compounds**
- 5. X-ray powder diffraction of compounds**
- 6. Crystalline Structure Analysis of Compounds**
- 7. Crystalline data of compounds**
- 8. Thermogravimetric analysis**
- 9. Solid-State Photochromic properties**
- 10. Solid-State Photoluminescence properties**
- 11. Magnetic properties**

1. Experiment instruments and reagents

The reagents used in the experiments were purchased from Sinopharm Group Co., Ltd., all of which were of analytical grade and were not further purified when used. The microwave heating instrument uses MAS-II microwave heating extraction workstation of Shanghai Xinyi Co., Ltd. Infrared spectroscopy was performed using a PerkinElmer Spectrum Two FT-IR infrared spectrometer with a potassium bromide tableting method with a scan range of 400-4000 cm^{-1} . Single crystal diffraction using Bruker Apex II single crystal diffractometer using a SMART APEX-II CCD detector with Mo $K\alpha$ ($\lambda = 0.71073 \text{ \AA}$). Crystals were kept at 296.15 K during data collection. Using Olex2, the structures were solved with the ShelXT structure solution program using Intrinsic Phasing and refined with the ShelXL refinement package using Least Squares minimization. PXRD was measured by a Bruker D8 Advance powder X-ray diffractometer with the Cu $K\alpha$ ray as a radiation source ($\lambda = 1.54056 \text{ \AA}$) and $90^\circ \geq 2\theta \geq 5^\circ$. Photoluminescence properties were measured by EDINBURGH FLS 980 fluorescence spectrophotometer with a monochromated 325 W Xe-arc excitation source and a visible detector (Hamamatsu R928P) and Hitachi F-7000 fluorescence spectrophotometer. UV-vis absorption spectrum was obtained with a TU-4100 spectrometer at room temperature. Thermogravimetric analysis using Swiss METTLER TOLEDO TGA/DSC3+ thermal analysis equipment. Magnetic susceptibility measurements were carried out with a S3Quantum Design SQUID (MPMS3 and PPMS-9) magnetometer in the temperature range of 1.8–310 K.

2. Synthesis of compounds

Microwave synthesis $\{[\text{Tm}_2(\text{H}_2\text{O})_{10}](\text{Mo}_8\text{O}_{27})\} \cdot 8\text{H}_2\text{O}$ (1-Tm)

Take 1.452 g (6.39 mmol) of $\text{Na}_2\text{MoO}_4 \cdot 2\text{H}_2\text{O}$, 0.401 g (1.26 mmol) of $\text{TmCl}_3 \cdot 7\text{H}_2\text{O}$ and 45 ml of water in a beaker with a volume of 50 ml. Then, 0.121 g (1 mmol) of THAM (Tris(hydroxymethyl)methyl aminomethane) was added, and the mixture was stirred at medium strength for 30 minutes to obtain white turbid system and pH about 8.5. The pH of the system was adjusted to 1.6 with $1 \text{ mol} \cdot \text{L}^{-1} \text{HClO}_4$ to obtain a nearly colorless solution. And then was 3.1 with $1 \text{ mol} \cdot \text{L}^{-1} \text{Na}_2\text{CO}_3$ solution. Then, the nearly colorless solution was heated under 600 watts microwave irradiation for 15 minutes, and the stirring speed was controlled at 300 r/min during the reaction. After completion of the reaction, colorless transparent solution was obtained. The solution was cooled to room temperature, after that, the mother liquor is obtained by filtration, and the mother liquor was allowed to stand for 2 days in the air to precipitate crystals. Yield: ca. 87.52% (based on $\text{Na}_2\text{MoO}_4 \cdot 2\text{H}_2\text{O}$). Anal. calcd (%) for $\{[\text{Tm}_2(\text{H}_2\text{O})_{10}](\text{Mo}_8\text{O}_{27})\} \cdot 8\text{H}_2\text{O}$: H, 1.53; Mo, 38.93; Tm, 23.99. Found: H, 1.55; Mo, 38.85; Tm, 23.87.

Alternatively, it was heated in a collector type magnetic stirring heater for 2 hours, and the obtained filtrate was allowed to stand for 20 days to precipitate crystals.

Microwave synthesis $\{[\text{Er}_2(\text{H}_2\text{O})_{10}](\text{Mo}_8\text{O}_{27})\} \cdot 8\text{H}_2\text{O}$ (2-Er)

The synthesis of compound **2-Er** is similar to **1-Tm** except that $\text{TmCl}_3 \cdot 7\text{H}_2\text{O}$ is replaced by the same molar amount (1.26 mmol) of $\text{ErCl}_3 \cdot 6\text{H}_2\text{O}$. Yield: ca. 85.32% (based on $\text{Na}_2\text{MoO}_4 \cdot 2\text{H}_2\text{O}$). Anal. calcd (%) for $\{[\text{Er}_2(\text{H}_2\text{O})_{10}](\text{Mo}_8\text{O}_{27})\} \cdot 8\text{H}_2\text{O}$: H, 1.54; Mo, 39.02; Er, 23.81. Found: H, 1.59; Mo, 38.97; Er, 23.79.

Similarly, compound **2-Er** also can be obtained by aqueous solution method.

3. Infrared spectroscopy analysis of compounds

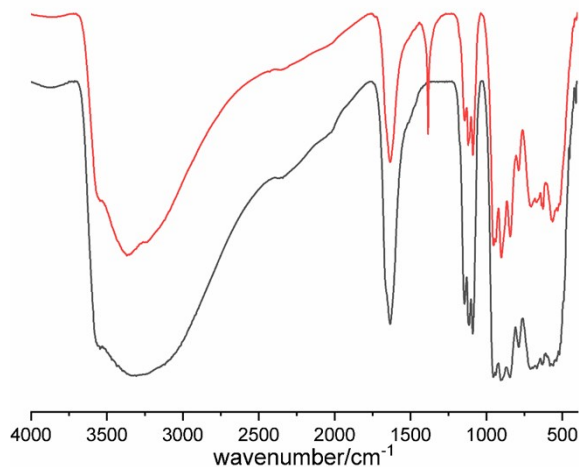


Figure S1. Infrared spectrum of compounds. The black line is the infrared spectrum of **1-Tm**, and the red line is the infrared spectrum of **2-Er**.

The infrared spectra of these two POMs were identical, indicating that they are isomorphous compounds.

The peaks of 949.61, 899.99 and 847.33 cm^{-1} are attributed to the stretching vibration of $\nu(\text{Mo}=\text{O})$; The peaks at 788.19, 706.32, 632.03 and 567.07 cm^{-1} are assigned to $\nu(\text{Mo}-\text{O}-\text{Mo})$; The peaks of 1143.06, 1114.33 and 1091.03 cm^{-1} are assigned to $\nu(\text{RE}-\text{O})$; The peaks appearing at 3327.64 and 1634.51 cm^{-1} correspond to the stretching vibration and bending vibration of water molecules.

4. UV-Vis spectroscopy of compounds

The UV-visible spectra of the compounds **1-Tm** and **2-Er** in aqueous solution are the same in the range of 200-800 nm.

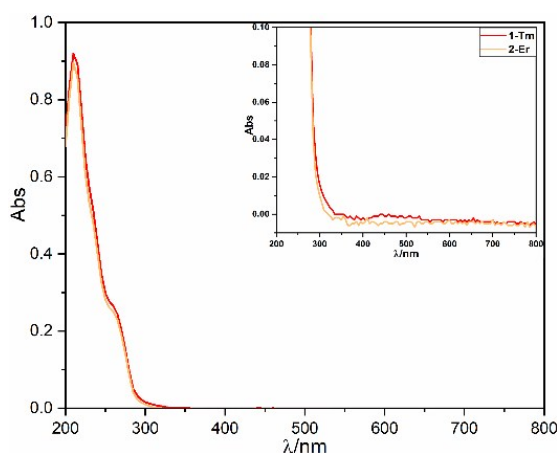


Figure S2. Ultraviolet-visible spectroscopy of compounds **1-Tm** and **2-Er** in aqueous solution at 200-800 nm.

There are two characteristic peaks at 200-400 nm, suggesting the presence of polyanions. The higher energy band at 210 nm is mainly owing to the $\pi\pi\text{-}d\pi$ charge transfer transition of the $\text{O}_t\rightarrow\text{Mo}$ bond. The relatively low absorption band is around 265 nm and can be attributed to the $\pi\pi\text{-}d\pi$ charge transfer transition of the $\text{O}_{b,c}\rightarrow\text{Mo}$ bond.

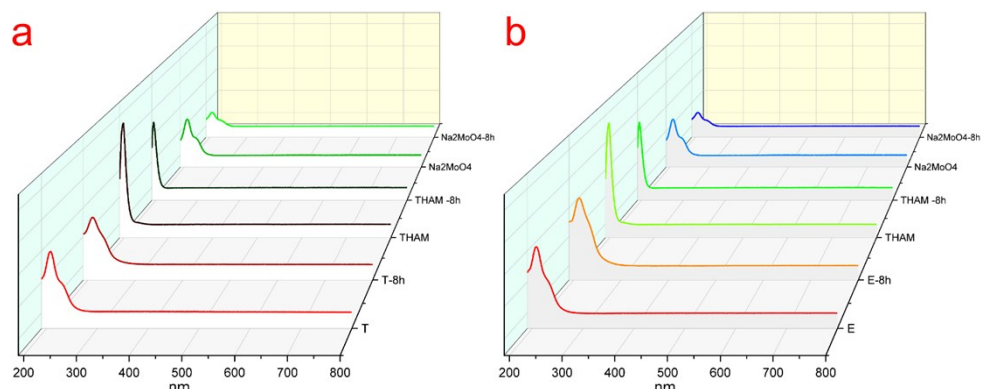


Figure S3. Ultraviolet-visible spectrum of compounds **1-Tm** (a) and **2-Er** (b) and their reaction materials THAM and sodium molybdate in aqueous solutions. After placed for about 8 hours in aqueous solutions another ultraviolet-visible spectrum of them also were obtained.

After placed for about 8 hours in aqueous solutions, the position of the absorption peaks in the UV-visible spectrum of **1-Tm** and **2-Er** are the same indicate that these two compounds are stable in water. The peaks of sodium molybdate change indicate that polymerization may have been occur in water. Both **1-Tm** and **2-Er** have the strongest absorption peaks at 210 nm and which are assigned to charge transfer transitions of terminal oxygen to Mo ($\text{O}_t\rightarrow\text{Mo}$) in the anion. Both **1-Tm** and **2-Er** have one weak absorption peak at 265 nm, which attributed to the $\text{O}_{b,c}\rightarrow\text{Mo}$ charge transfer. THAM (Tris(hydroxymethyl)methyl aminomethane) has only one strong absorption peak at 200 nm, sodium molybdate has two absorption peaks at 210 nm and 265 nm.

5. X-ray powder diffraction of compounds

In order to verify the phase purity of samples which used for the experiments, X-ray powder diffraction of these two compounds were done separately and compared with simulated data from single crystal X-ray diffraction.

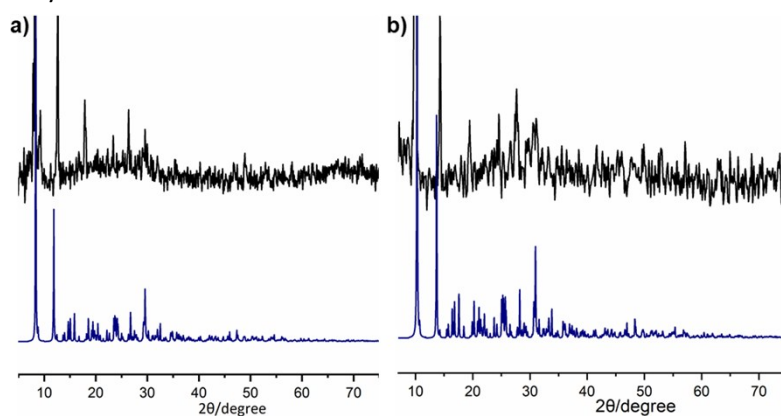


Figure S4. (a) The PXRD spectrum of **1-Tm**, (b) the PXRD spectrum of **2-Er**. The black lines are the

experimental results, the blue lines are the simulated results obtained from the single crystal data.

The phase purity of these two samples have been checked by comparing the X-ray powder diffraction spectrum of experimental results and the simulated results obtained from the single crystal data. Differences in intensity of experiments and simulated PXRD may be due to changes in the preferred orientation of the powder samples during the collection of experimental data.

6. Crystalline Structure Analysis

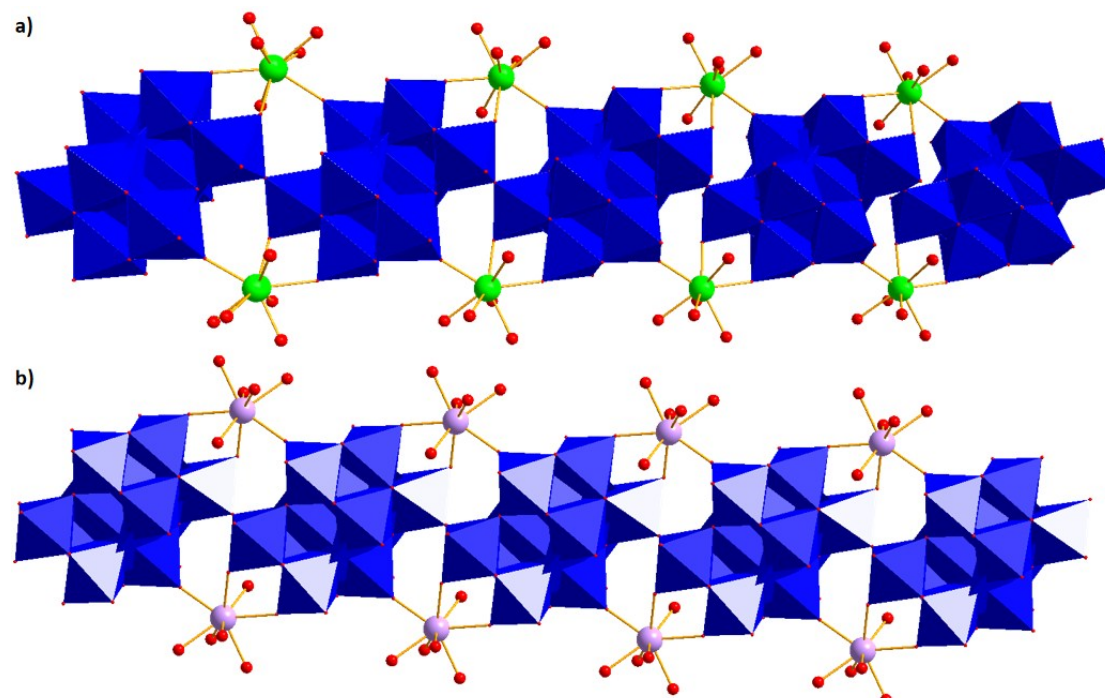


Figure S5. (a,b) polyhedral diagram of **1-Tm** and **2-Er**. Mo, blue; O, red; Tm, green; Er, pink.

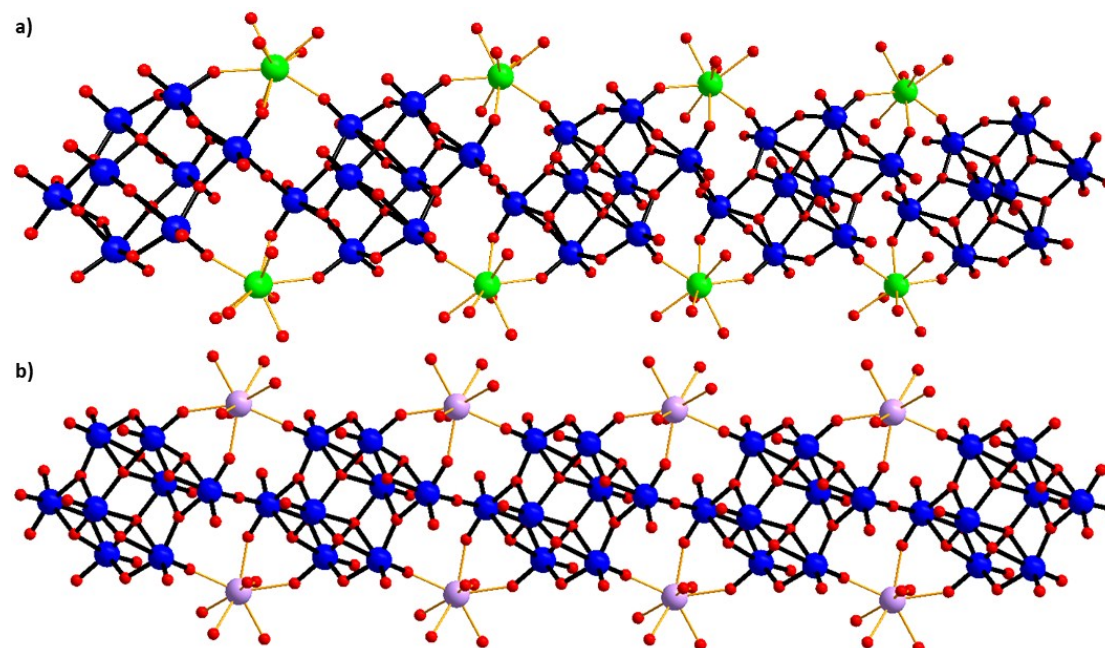


Figure S6. (a,b) ball-stick diagram of **1-Tm** and **2-Er**. Mo, blue; O, red; Tm, green; Er, pink.

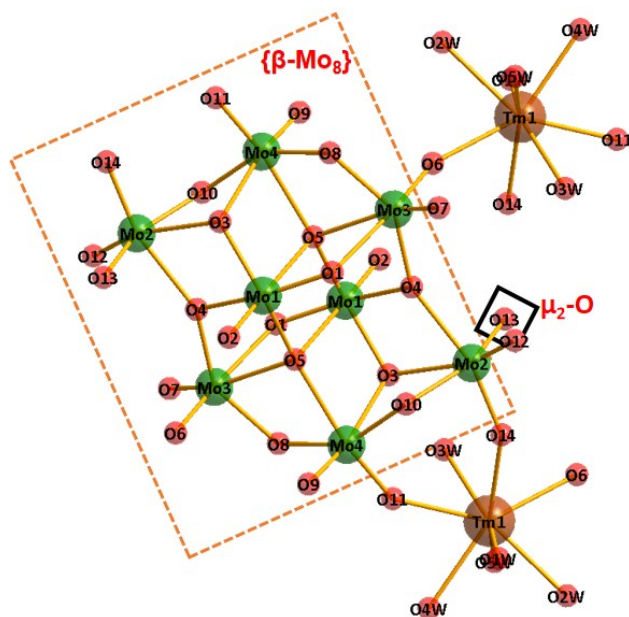


Figure S7. Atomic connection of compound **1-Tm**. (**2-Er** is similar to **1-Tm**.)

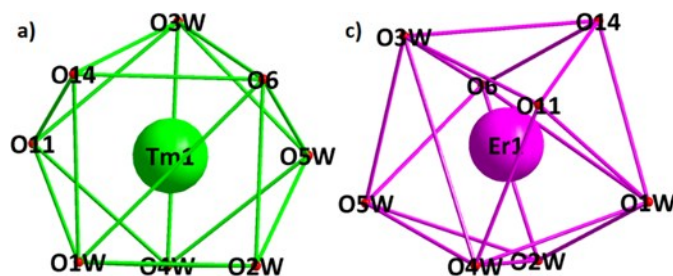


Figure S8. (a) coordination environments of lanthanide ion Tm^{3+} in **1-Tm**. (b) coordination environments of lanthanide ion Er^{3+} in **2-Er**.

In compound **1-Tm**, lanthanide ions Tm^{3+} are coordinated with eight O atoms by eight-coordinate mode. The bond lengths of Tm1-O6 is 2.3236(46) Å, Tm1-O11 is 2.3898(41) Å and Tm1-O14 is 2.3100(42) Å, they are longer than the average bond length of Tm-O . This is due to these three oxygen atoms ($\mu_2\text{-O6}$, O11 and O14) coordinate with Mo atoms. Where the bond lengths of Mo2-O14 is 1.7647(45) Å, Mo3-O6 is 1.7436(40) Å and Mo4-O11 is 1.7404(45) Å. They are longer than the average Mo-O bond due to these three oxygen atoms also coordinate with Tm^{3+} ions. The bond angle of Mo2-O14-Tm1 is $146.695(226)^\circ$, Mo3-O6-Tm1 is $153.041(247)^\circ$, and the bond angle of Mo4-O11-Tm1 is $147.202(215)^\circ$, respectively.

Similarly, in compound **2-Er**, lanthanide ions Er^{3+} are also coordinated with eight O atoms by eight-coordinate mode. The bond lengths of Er1-O6 is 2.3407(67) Å, Er1-O11 is 2.3977(71) Å and Er1-O14 is 2.3350(75) Å, respectively. They are also longer than the average bond length of Er-O . This is due to these three oxygen atoms coordinate with Mo atoms. Where, the bond lengths of Mo2-O14 is 1.7447(78) Å, Mo3-O6 is 1.7314(68) Å and Mo4-O11 is 1.7388(79) Å, respectively. They are also longer than the average Mo-O bond, due to these three oxygen atoms coordinate with Er^{3+} ions. The bond angle of Mo2-O14-Er1 is $146.824(379)^\circ$, Mo3-O6-Er1 is $153.420(415)^\circ$, and the bond angle of Mo4-O11-Er1 is $147.056(376)^\circ$, respectively.

7. Crystalline data of compounds

Table S1. Crystal data and structure refinement for **1-Tm** and **2-Er**.

Identification code	1-Tm	2-Er
Empirical formula	Mo ₈ O ₄₅ H ₂₀ Tm ₂	Mo ₈ O ₄₅ H ₂₀ Er ₂
Formula weight	1825.38	1822.04
Temperature/K	296.15	296.15
Crystal system	triclinic	triclinic
Space group	P-1	P-1
a/Å	9.2867(7)	9.2905(12)
b/Å	10.2931(8)	10.3007(13)
c/Å	10.7281(8)	10.7373(14)
α/°	90.6230(10)	90.642(2)
β/°	99.0190(10)	98.969(2)
γ/°	102.6890(10)	102.623(2)
Volume/Å ³	986.98(13)	989.4(2)
Z	1	1
ρ _{calc} /g/cm ³	3.071	3.058
μ/mm ⁻¹	7.018	6.758
F(000)	834.0	832.0
Crystal size/mm ³	0.23 × 0.18 × 0.15	0.21 × 0.17 × 0.15
Radiation	MoKα (λ = 0.71073)	MoKα (λ = 0.71073)
2θ range for data collection/°	4.06 to 50.192	4.056 to 50.198
Index ranges	-10 ≤ h ≤ 11, -9 ≤ k ≤ 12, -12 ≤ l ≤ 12	-11 ≤ h ≤ 11, -7 ≤ k ≤ 12, -12 ≤ l ≤ 12
Reflections collected	5070	5117
Independent reflections	3463 [R _{int} = 0.0165, R _{sigma} = 0.0302]	3493 [R _{int} = 0.0267, R _{sigma} = 0.0541]
Data/restraints/parameters	3463/0/249	3493/0/249
Goodness-of-fit on F ²	1.054	0.869
Final R indexes [I ≥ 2σ (I)]	R ₁ = 0.0256, wR ₂ = 0.0669	R ₁ = 0.0398, wR ₂ = 0.1067
Final R indexes [all data]	R ₁ = 0.0269, wR ₂ = 0.0677	R ₁ = 0.0532, wR ₂ = 0.1189
Largest diff. peak/hole / e Å ⁻³	2.04/-0.81	2.21/-1.33

^a $R_1 = \sum ||F_o| - |F_c|| / \sum |F_o|$. ^b $wR_2 = \{\sum [w(F_o^2 - F_c^2)^2] / \sum [w(F_o^2)^2]\}^{1/2}$

Table S2. Bond valence sum parameters for Mo and Tm atoms in **1-Tm**

Bond	Bond length	Bond Valence	Valence Sum
Tm1-O6 ¹	2.323	0.417708	$\Sigma(\text{Tm1}) = 3.205093$
Tm1-O11	2.389	0.349465	
Tm1-O14	2.31	0.432645	
Tm1-O1W	2.335	0.404378	
Tm1-O2W	2.361	0.376938	
Tm1-O3W	2.299	0.4457	
Tm1-O4W	2.326	0.414335	
Tm1-O5W	2.374	0.363924	
Mo1-O1	1.744	1.553547	
Mo1-O2	1.704	1.730912	
Mo1-O3	1.876	1.087394	
Mo1-O4	2.162	0.501983	
Mo1-O5	1.958	0.87124	
Mo1-O5 ²	2.471	0.217768	
Mo2-O3 ²	2.322	0.325751	$\Sigma(\text{Mo2}) = 6.010494$
Mo2-O4 ²	2.12	0.562325	
Mo2-O10	1.982	0.816521	
Mo2-O12	1.696	1.768745	
Mo2-O13	1.8822	1.069324	
Mo2-O14	1.765	1.467828	
Mo3-O1 ²	2.332	0.317065	$\Sigma(\text{Mo3}) = 6.042132$
Mo3-O4	1.909	0.994609	
Mo3-O5	2.206	0.4457	
Mo3-O6	1.744	1.553547	
Mo3-O7	1.695	1.773532	
Mo3-O8	1.923	0.957678	
Mo4-O3 ²	2.283	0.361962	$\Sigma(\text{Mo4}) = 5.994954$
Mo4-O5	2.202	0.450545	
Mo4-O8	1.982	0.816521	
Mo4-O9	1.703	1.735597	
Mo4-O10	1.884	1.064135	
Mo4-O11	1.741	1.566194	

Table S3. Bond valence sum parameters for Mo and Er atoms in **2-Er**

Bond	Bond length	Bond Valence	Valence Sum
Er1-O6 ¹	2.341	0.408773	$\Sigma(\text{Er1}) = 3.185012$
Er1-O11	2.397	0.351359	
Er1-O14	2.335	0.415456	
Er1-O1W	2.346	0.403286	
Er1-O2W	2.366	0.382066	
Er1-O3W	2.319	0.433816	
Er1-O4W	2.336	0.414335	
Er1-O5W	2.372	0.37592	
Mo1-O1	1.739	1.574683	$\Sigma(\text{Mo1}) = 5.998397$
Mo1-O2	1.711	1.698473	
Mo1-O3	1.86	1.135448	
Mo1-O4	2.159	0.50607	
Mo1-O5	1.96	0.866543	
Mo1-O5 ²	2.472	0.21718	
Mo2-O3 ²	2.315	0.331973	$\Sigma(\text{Mo2}) = 6.125653$
Mo2-O4 ²	2.123	0.557784	
Mo2-O10	1.981	0.818731	
Mo2-O12	1.689	1.802526	
Mo2-O13	1.8836	1.065286	
Mo2-O14	1.745	1.549354	
Mo3-O1 ²	2.328	0.320511	$\Sigma(\text{Mo3}) = 6.130974$
Mo3-O4	1.909	0.994609	
Mo3-O5	2.206	0.4457	
Mo3-O6	1.732	1.604758	
Mo3-O7	1.689	1.802526	
Mo3-O8	1.921	0.962869	
Mo4-O3 ²	2.29	0.355178	$\Sigma(\text{Mo4}) = 5.981665$
Mo4-O5	2.2	0.452987	
Mo4-O8	1.987	0.805561	
Mo4-O9	1.705	1.726241	
Mo4-O10	1.883	1.067015	
Mo4-O11	1.739	1.574683	

8. Thermogravimetric analysis

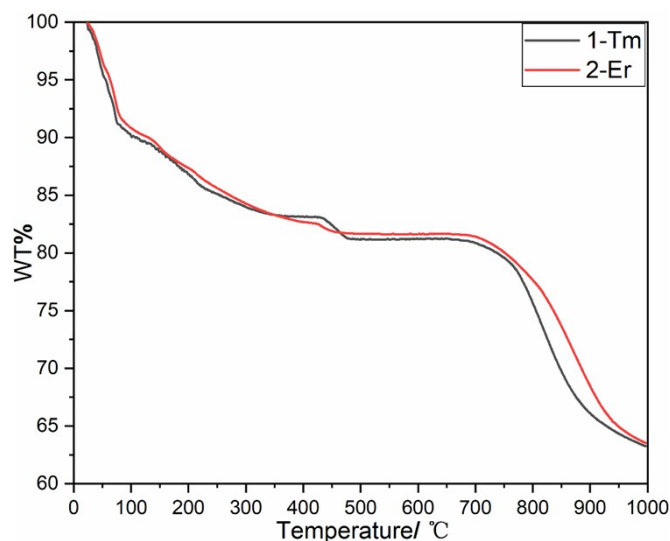


Figure S9. Thermogravimetric analysis of compound **1-Tm** showed that the sample lost 8.68% before 100 °C, corresponding to the loss of 8 free water molecules. Then, as the temperature increases, the sample continue lose weight, possibly due to the structure of the compound slow decomposition. The thermal stability of **2-Er** is the same as **1-Tm**.

9. Solid-State Photochromic properties

Photochromic experiment: Sample powders were evenly spread on a white ceramic test plate. The xenon lamp has an operating current of 5 amps and the distance of 5 centimeters to the samples. In order to stabilize the light and the environment, the xenon lamp was turned on and adjusted before experiment. After 10 minutes, the light was in a steady state.

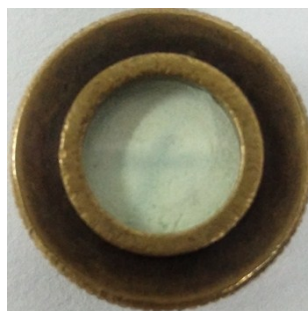


Figure S10. Occasionally observed photochromic behavior of **1-Tm**

After the photoluminescence spectrum of sample **1-Tm** was measured, a dark line was observed on the sample piece. In order to determine the cause of the dark line, the sample sheet was rotated for 90 degrees. Then the test was performed again, and another dark line was produced at 90 degrees from the original position. It is inferred that the dark lines may be due to the ultraviolet irradiation during photoluminescence process.



Figure S11. Temperature influence exclusion experiment device

Considering that samples were irradiated with Xe lamp, the temperature due to irradiation may interfere with the result of photochromism. Control irradiation distance and other conditions were the same as photochromic process to make a blank experiment. The room temperature was 20 °C and the current of xenon lamp was 5 amps. When the irradiation time was 5 minutes, the temperature of these two thermometers indicate were 25 °C and 23 °C. And when the irradiation time was 10 minutes, the temperature indicate were 41 °C and 40 °C. Finally, when the irradiation time was 30 minutes, the temperature indicate were 41°C and 40 °C, respectively. These phenomena indicate that even after a long-time (>30 minutes) irradiation, the temperature of the test area increased by no more than 20 °C. Therefore, temperature influence caused by irradiation can be ignored.

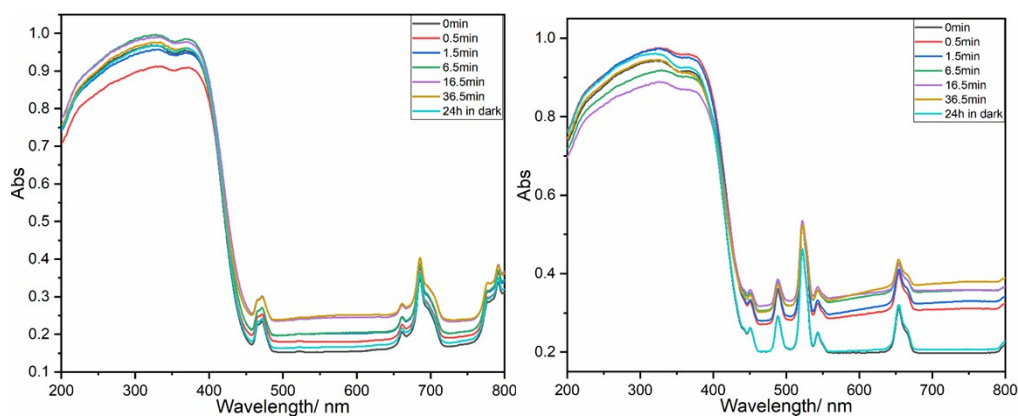


Figure S12. Solid-state UV-vis/diffuse absorbance spectra of **1-Tm** (left) and **2-Er** (right).

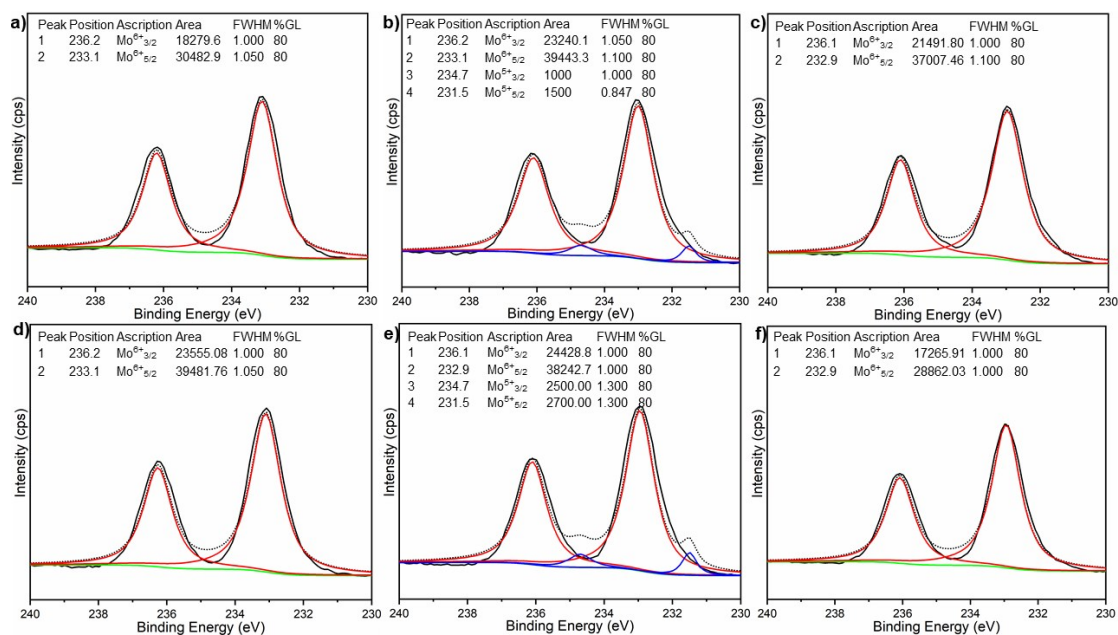


Figure S13. XPS Mo3d of **1-Tm** before irradiation (a), after 36.5 min of irradiation (b), and 24 hours in the dark (c); XPS Mo3d of **2-Er** before irradiation (d), after 36.5 min of irradiation (e), and 24 hours in the dark (f). Dotted lines correspond to the experimental results that can be deconvoluted into two pairs of peaks corresponding to Mo(VI) (red curves) and Mo(V) (blue curves). Fitting of the experimental results (black curves) by summation of the deconvoluted peaks.

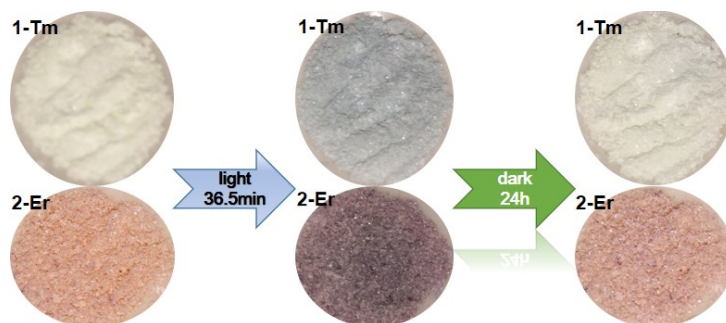


Figure S14. Coloration and fading of compounds **1-Tm** and **2-Er**.



Figure S15. (a,b) Photochromism and color retention experiments of compound **1-Tm**; (c,d) Photochromism and color retention experiments of compound **2-Er**.

10. Solid-State Photoluminescence properties

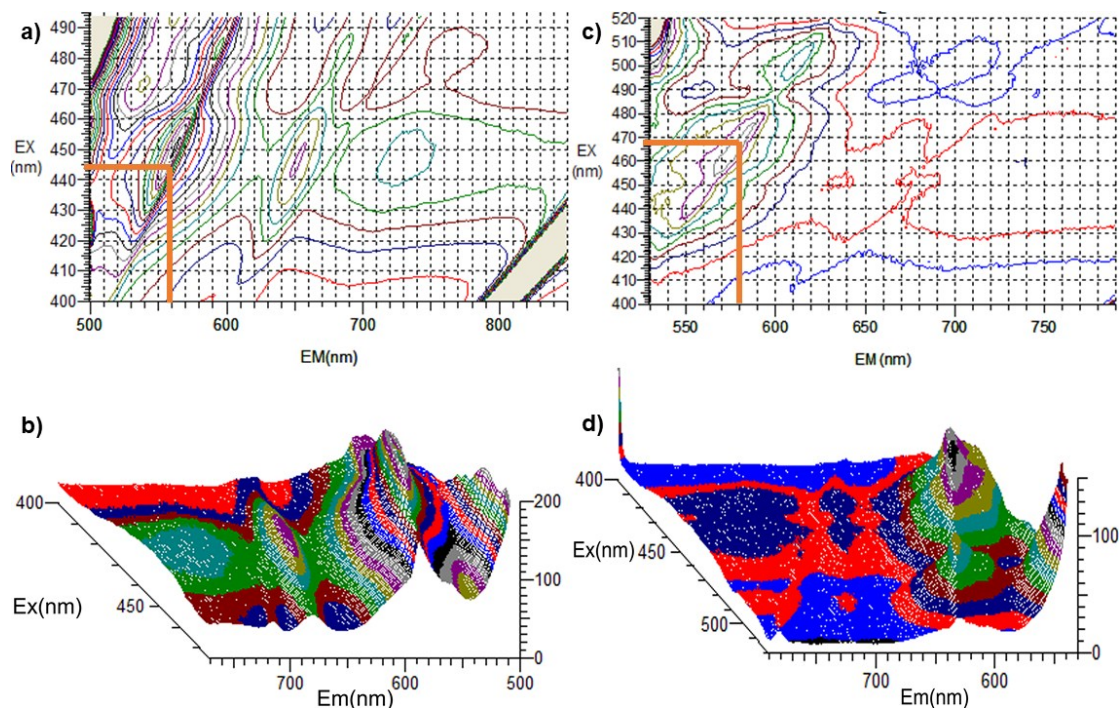


Figure S16. (a,b) Three-dimensional (3D) excitation/emission matrix fluorescence (EEMF) map and spectrum of **1-Tm**, respectively, (c,d) three-dimensional (3D) excitation/emission matrix fluorescence (EEMF) map and spectrum of **2-Er**, respectively.

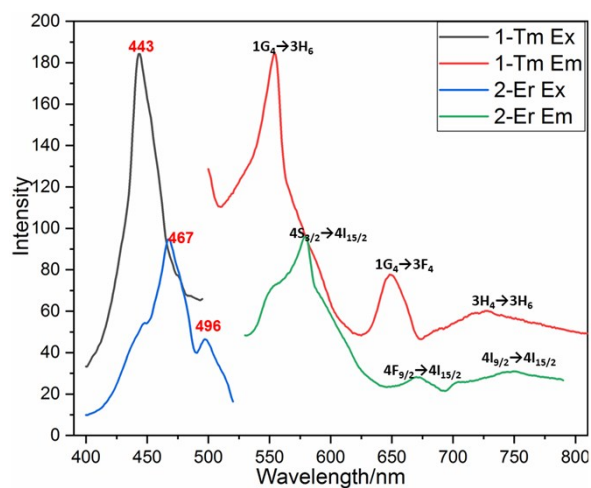


Figure S17. Two-dimensional photoluminescence excitation and emission spectrum of compounds **1-Tm** and **2-Er**.

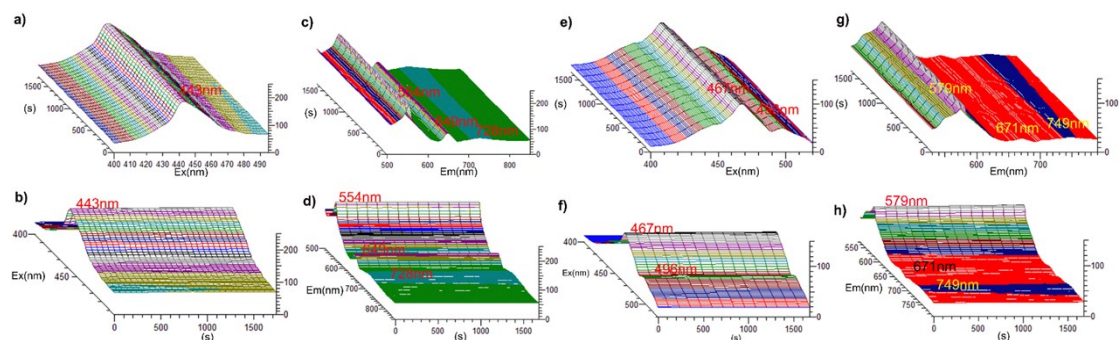


Figure S18. (a,b) show the compound **1-Tm** has the most intense excitation peak at 443 nm, the intensity and position of the excitation peak did not change from 0 s to 1800 s. (c,d) show compound **1-Tm** has three emission peaks at 554 nm, 649 nm and 728 nm under 443 nm photoexcitation. The intensity and position of these emission peaks did not change from 0s to 1800s. (e,f) show compound **2-Er** has two excitation peaks at 467 nm and 496 nm. The intensity and position of these excitation peaks did not change from 0s to 1800s. (g,h) show compound **2-Er** has three emission peaks at 579 nm, 671 nm and 749 nm under 467 nm photoexcitation. The intensity and position of these emission peaks did not change from 0s to 1800s.

Time-based 3D-time scan spectrum of these two compounds indicate that the peaks position and intensity of the luminescence with the irradiation time extension (0-1800 s or longer) did not change. It is shown that the electrons of Tm^{3+} and Er^{3+} ions are transferred from the ground state to the excited states after they absorb energy, and then the excited electrons relax to the lower energy level by a radiative process are stable. It is also indicate that the photoluminescence ability of these two compounds are stable.

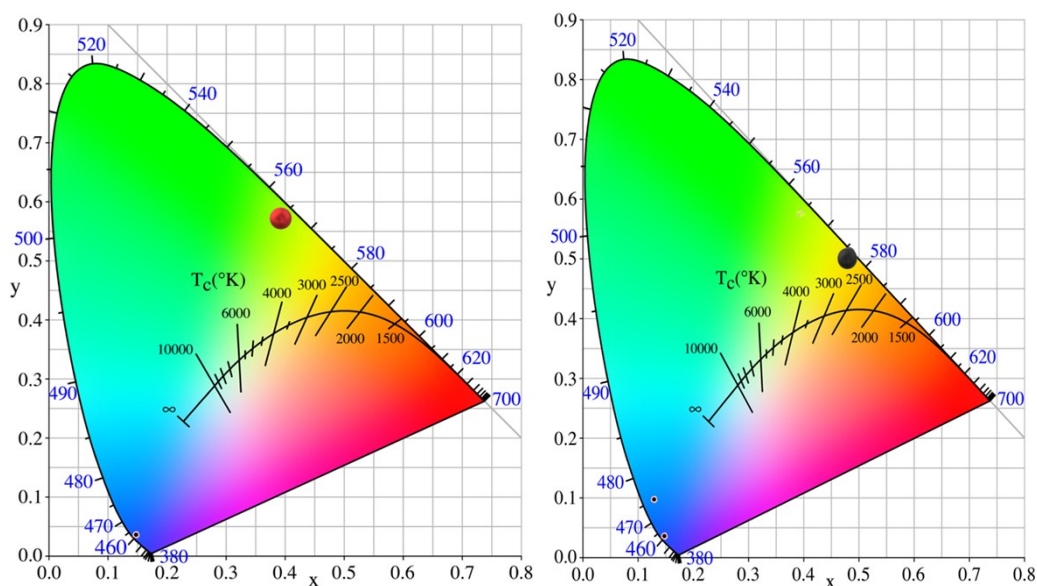


Figure S19. The CIE 1931 chromaticity diagrams of the emissions of **1-Tm** and **2-Er**.

11. Magnetic properties

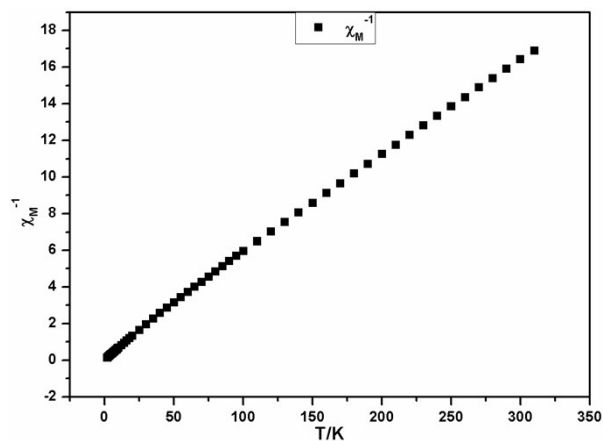


Figure S20. $1/\chi_M$ versus T plots of **1-Tm** in the 1.8–310 K range.

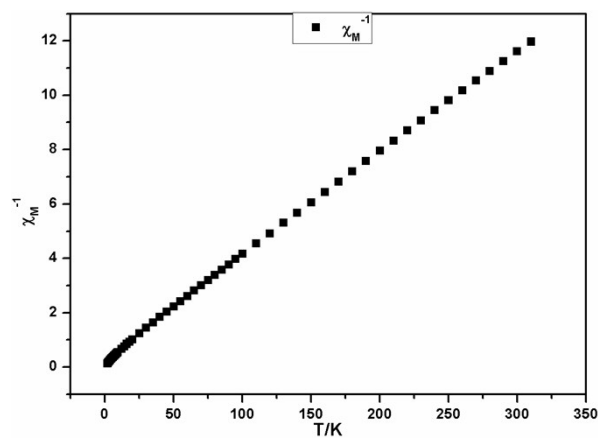


Figure S21. $1/\chi_M$ versus T plots of **2-Er** in the 1.8–310 K range.

In all the samples there is a linear part of the inverse susceptibility curve that follows the Curie–Weiss law ($\chi = C/(T - \theta)$ where C is the Curie constant and θ is the Weiss temperature).

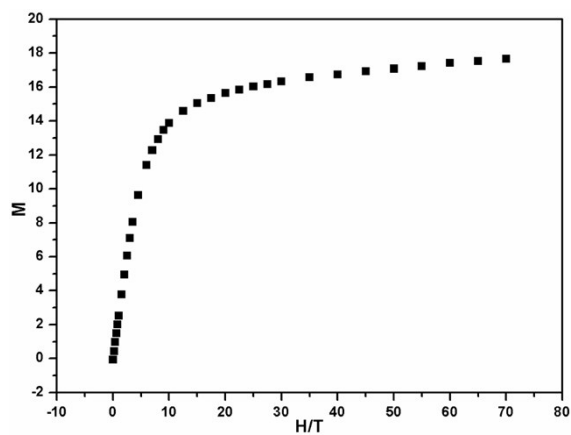


Figure S22. The magnetic field (H) dependence magnetization (M) curves for **1-Tm**.

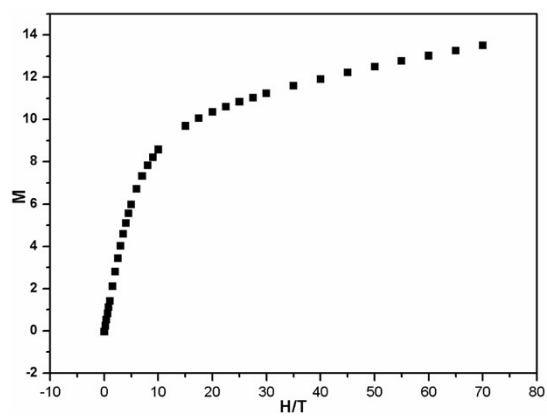


Figure S23. The magnetic field (H) dependence magnetization (M) curves for **2-Er**.